



ELSEVIER

Combustion and Flame 134 (2003) 327–337

Combustion
and Flame

A computational study of oscillatory extinction of spherical diffusion flames

Erik W. Christiansen^a, Stephen D. Tse^b, Chung K. Law^{a,*}

^a*Department of Mechanical and Aerospace Engineering, Princeton University, Princeton, NJ 08544, USA*

^b*Department of Mechanical and Aerospace Engineering, Rutgers, the State University of New Jersey, Piscataway, NJ 08854, USA*

Received 1 April 2002; received in revised form 28 January 2003; accepted 24 March 2003

Abstract

The transient behavior of burner-supported spherical diffusion flames was studied in the transport-induced limit of low mass flow rate and the radiation-induced limit of high mass flow rate which characterize the isola response of flame extinction. Oscillatory instability was observed near both steady-state extinction limits. The oscillation typically grows in amplitude until it becomes large enough to extinguish the flame. The oscillatory behavior was numerically observed using detailed chemistry and transport for methane (50%CH₄/50%He into 21%O₂/79%He) and hydrogen (100% H₂ into 21%O₂/79%He) diffusion flames where the fuel was issued from a point source, and helium was selected as an inert to increase the Lewis number, facilitating the onset of oscillation. In both methane and hydrogen flames, the oscillation always leads to extinction, and no limit cycle behavior was found. The growth rate of the oscillation was found to be slow enough under certain conditions to allow the flame to oscillate for over 450 s, suggesting that such oscillations can possibly be observed experimentally. For the hydrogen flames, however, the frequency of oscillation near the transport-induced limit is much larger, approximately 60 Hz as compared to 0.35 Hz for the methane flame, and the maximum amplitude of temperature oscillations was about 5 K. The distinctively different structures of the hydrogen and methane flames suggest that while both instabilities are thermal-diffusive in origin, oscillations in the hydrogen flames resemble those of premixed flames, while oscillations in the methane flames are non-premixed in character. © 2003 The Combustion Institute. All rights reserved.

Keywords: Diffusion flames; Oscillating flames; Extinction

1. Introduction

Steady-state analysis demonstrates that extinction in diffusion flames is achieved when the Damköhler number (Da) becomes sufficiently small, where Da is defined as the ratio of the characteristic residence time through the flame to the characteristic chemical reaction time. Extinction is characterized by exces-

sive leakage of the fuel and oxidizer through the flame front, as there is insufficient time for complete reaction. For a spherically symmetric diffusion flame in which the fuel is introduced from a point source, low Damköhler number extinction can be achieved via two different mechanisms. For low mass flow rates (m), the flame radius (r_f) is small (since $r_f \sim m$) and the reaction zone situates itself in a region of high flow velocity (since $v \sim 1/r^2$). This high velocity through the flame corresponds to a short residence time in the reaction zone, which facilitates transport-induced extinction in the manner described above.

* Corresponding author. Tel.: +1-609-258-5271; Fax: +1-609-258-6233.

E-mail address: cklaw@princeton.edu (C.K. Law).

On the other hand, if the mass flow rate is increased, the flame burns stronger and the flame radius also increases. However, as the flame increases in size, the heat loss due to radiation also increases due to the increased volume of the flame. The increased heat loss due to radiation eventually lowers the flame temperature and increases the chemical reaction time to such an extent that radiation-induced extinction is achieved. These two phenomena are responsible for the isola-shaped response of spherical diffusion flames, with either gas-phase [1,2] or surface [3] radiative heat loss.

The above discussion of extinction limits is based on steady-state analysis. However, it is not unreasonable to expect that extinction could occur in an unsteady manner. Indeed, near-limit oscillations have been observed experimentally under microgravity conditions for candle flames [4] as well as droplet flames [5]. In both cases, approximately five to eight oscillations were observed with a frequency of about 1 Hz before the flame extinguished. More recently, pulsating behavior was observed under normal gravity conditions in a jet flame configuration by Fűri et al. [6]. Oscillations were induced by reducing the oxygen concentration in propane and methane flames diluted with both nitrogen and helium.

There have been several analytical studies on the oscillatory stability of diffusion flames. Kirkby and Schmitz [7] showed analytically that oscillations may develop in near-limit diffusion flames of non-unity Lewis number ($Le = \lambda/\rho c_p D$). Kim [8] used activation-energy asymptotics to study the stability of non-unity Lewis number diffusion flames, based on the canonical diffusion flame structure of Liñán [9]. His results show the development of cellular instability for $Le < 1$, and pulsating instability for $Le > 1$, which is similar to the well-known diffusional-thermal instability in premixed flames [10]. Cheatham and Matalon [11] analytically investigated the unsteady behavior of droplet diffusion flames in the presence of heat loss. They were able to identify an oscillatory regime in flames that could be triggered by either a sufficiently large Lewis number (even without heat loss) or by appreciable heat loss (even for $Le = 1$). Additionally, the frequency of oscillation for typical diffusion flames that could be prone to oscillation was estimated to be in the range of 0.5–5 Hz. Kukuck and Matalon [12] extended this analysis, using a planar configuration, to investigate the effects of mixture strength, temperature differential between the supply streams, and volumetric heat loss on the stability boundaries.

Sohn and coworkers numerically investigated the unsteady response of a one-dimensional planar chambered diffusion flame using an adiabatic, non-unity Lewis number formulation [13] as well as one with

unity Lewis number and radiative heat loss [14], employing a two-reactant, one-step chemistry model. For the adiabatic case [13] oscillation leading to extinction in near-limit flames was observed, but limit cycles were not found. When radiative heat loss was taken into account [14], the isola response was observed in steady-state calculations. Oscillatory instability leading to extinction was observed near both turning points of the isola. Additionally, an extremely small regime in Da was identified where stable limit cycles exist near the radiation-induced limit.

It is significant to note that all of the above studies, analytical as well as computational, have adopted simplified descriptions of chemistry and transport. However, recent studies on flames have amply demonstrated that such assumptions could yield results that could be quantitatively inaccurate as well as qualitatively mal-descriptive. For example, using detailed descriptions of transport and chemistry, it was shown [15] that the tendency for hydrogen/air premixed flames to undergo oscillatory burning can vary non-monotonically with increasing pressure, a result that can not be captured by using one-step chemistry, and that diffusional-thermal pulsating instability can promote extinction before the flammability predicted by steady-state calculations is reached [15–17].

In view of the above considerations, in the present investigation we have performed a computational study of the pulsating instability of one-dimensional diffusion flames with radiative heat loss, using detailed chemistry and transport in order to observe the oscillations in real systems, and to investigate the influence of the flame structure on the instability. The spherical geometry was chosen because it is the only one-dimensional steady-state diffusion flame configuration with unbounded boundary. Additionally, by introducing the fuel mixture into the domain in the gaseous phase at a fixed mass flow rate through a point source, any feedback between the flame and the fuel source that could exist in a droplet flame and obscure the mechanism responsible for the oscillation was eliminated. Two different mixtures were used in the study, in our study, with helium as a diluent in order to achieve non-unity Lewis numbers: 50%CH₄/50%He into 21%O₂/79%He and 100%H₂ into 21%O₂/79%He. The former mixture is characterized by $Le > 1$ for both the fuel ($Le = 2.3$) and the oxidizer (1.9), while in the latter mixture, $Le < 1$ for the fuel (0.3) and $Le > 1$ for the oxidizer (1.9). These two cases have been chosen in order to clearly identify the role of non-equidiffusion in promoting the instability, as predicted by theory, e.g. Ref [12]. Note that the values of Le given are estimated from the free stream values, simply as a point of reference, given that the methodology does not exist to extract quantitatively and rigorously such properties for (variable

property, detailed transport, multi-step reaction, fully transient) diffusion flames. The work complements previous theoretical studies but extends far beyond by examining nonlinear effects inherent in the developing oscillations and transient extinction. Results obtained from these specific mixtures also assist us in the planning of microgravity experiments.

The numerical methodology employed in this investigation will be discussed, followed by presentation of the results along with discussion of the behavior observed.

2. Numerical methodology

The spherically symmetric unsteady diffusion flame was simulated using an appropriately modified version of the flame code developed by Kee et al. [18]. The governing equations for global mass conservation, species conservation, and energy conservation (including radiative heat loss) are as follows:

$$\rho A \frac{\partial}{\partial t} + \frac{\partial m}{\partial r} = 0$$

$$\rho A \frac{\partial Y_k}{\partial t} + m \frac{\partial Y_k}{\partial r} + \frac{\partial}{\partial r} (\rho A Y_k V_k) - A \omega_k W_k = 0$$

$$\begin{aligned} \rho A \frac{\partial T}{\partial t} + m \frac{\partial T}{\partial r} - \frac{1}{c_p} \frac{\partial}{\partial r} \left(A \lambda \frac{\partial T}{\partial r} \right) \\ + \frac{1}{c_p} \sum_{k=1}^K \rho A Y_k V_k c_{p,k} \frac{\partial T}{\partial r} + \frac{1}{c_p} \sum_{k=1}^K A \omega_k h_k W_k \\ + A \frac{q}{c_p} = 0 \end{aligned}$$

where r is the radial coordinate, $A = 4\pi r^2$ the surface area of a shell with radius r , m the mass flow rate, T the temperature, K the total number of species, Y_k the mass fraction of the k th species, ρ the mass density, W_k the molecular weight, c_p and λ the constant pressure heat capacity and the thermal conductivity of the mixture, ω_k the molar rate of chemical production per unit volume, h_k the specific enthalpy, V_k the diffusion velocity, and q the radiative heat loss per unit volume. The flame was assumed to be optically thin, so that the volumetric heat loss term is given by:

$$q = 4\alpha_p \sigma (T^4 - T_u^4)$$

where σ is the Stefan-Boltzmann constant and α_p the total Planck mean absorption coefficient. Radiative heat loss from CO, CO₂, and H₂O was considered in the calculations. The temperature dependent functions for α_{CO} , α_{CO_2} , and $\alpha_{\text{H}_2\text{O}}$ were taken from Ref. [19].

For the methane flames, the detailed reaction mechanism employed was GRI Mech1.2 [20], which consists of 31 species and 175 reaction steps. In the case of the hydrogen flames, the reaction mechanism was taken from Mueller et al. [21], which consists of 9 species and 21 reaction steps. Adaptive re-gridding in both time and space was utilized in order to fully resolve the details of the flame structure and its transitory response.

At $r = 0$, the boundary conditions imposed were a fixed mass flow rate m , temperature $T_o = 300$ K, and mass flux fractions $Y_k = \epsilon_k$, where ϵ_k is the mass fraction of the k th species of the initial mixture. At the ambience side, the boundary conditions imposed were temperature $T_\infty = 300$ K, and oxidizer composition (21% O₂/79% He). The ambient pressure was fixed at 1 atm. The computational domain was chosen to be sufficiently large (500 cm) so that the influence of the finite far boundary would be insignificant. The gradients were found to be negligibly small at the finite boundary of such a domain.

3. Results and discussion

3.1. Methane diffusion flames

3.1.1. Steady-state response

The steady-state response curve for the 50%CH₄/50%He fuel stream into the 21%O₂/79%He oxidizing environment was determined for both adiabatic flames and flames with radiative heat loss. The maximum flame temperature as a function of the mass flow rate is shown in Fig. 1. For the adiabatic flame, an extinction limit is reached as the mass flow rate (and hence Da) is decreased. This transport-induced extinction limit is characterized by a turning point which is marked by a circle on the curve. On the other hand, as the mass flow rate of the adiabatic flame is increased, the flame burns increasingly stronger. The effect of radiative heat loss on the flame response is negligible at low mass flow rates, and the two curves basically overlap and share the same turning point. However, at larger mass flow rates, the flame becomes larger in size and the heat loss due to radiation becomes increasingly significant. The flame radius increases proportionally to the mass flow rate, and hence the volume of the flame increases with the cube of the mass flow rate. Eventually, the heat loss due to radiation becomes sufficiently large to extinguish the curve. This radiation-induced extinction turning point is marked by the circle on the right hand side of the curve. The square points on either end of the curve just before extinction mark the onset of oscillation which is discussed next.

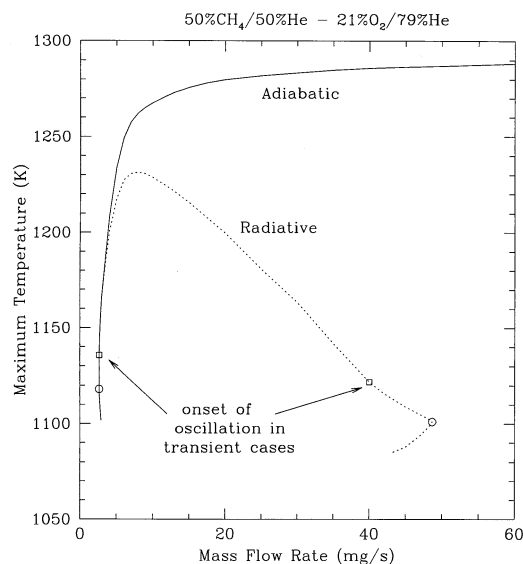


Fig. 1. Maximum temperature in steady-state methane diffusion flames vs. mass flow rate, both adiabatic and with radiative heat loss.

3.1.2. Transient response

Having determined the steady-state response of the methane diffusion flames, we then investigate the stability of these solutions by imposing a small (0.1%) perturbation to the temperature profile. We opted to perturb the temperature profile as opposed to the mass flow rate (as in Refs. [13,14]) so that the flame response would be unaffected by disturbances to the boundary conditions. Two distinct types of response were observed depending on the mass flow rate: 1) stable situation where the perturbation damps out and the flame approaches the steady-state solution in an oscillatory manner and 2) unstable situation where the perturbation grows until the amplitude of oscillation becomes large enough to extinguish the flame. Figure 2 illustrates these two different types of behavior near the transport-induced extinction limit for the methane diffusion flame. The maximum temperature is plotted vs. time for three mass flow rates: 2.68, 2.67, and 2.66 mg/s. It is seen that, for the largest mass flow rate, the initial perturbation is damped out after a few oscillations. Reducing the mass flow rate results in an oscillation that grows in amplitude over several cycles until the flame eventually extinguishes. Finally, further reducing the mass flow rate prompts extinction after just a few cycles. The frequency of oscillation is about 0.35 Hz, which is of the order of the frequency predicted by Refs. [11,12]. It is also worth noting that similar calculations were performed both with and without

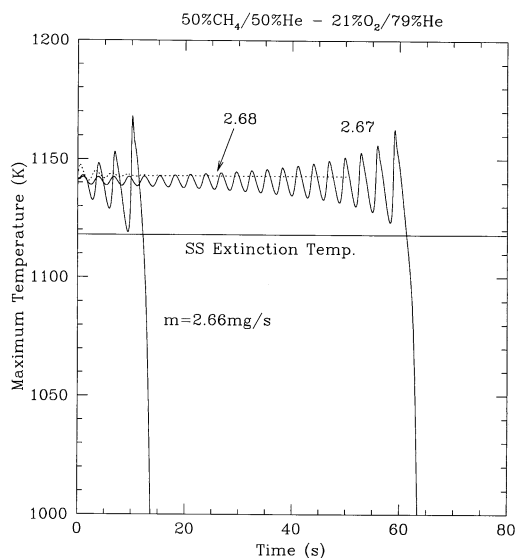


Fig. 2. Maximum temperature as a function of time for methane diffusion flames with mass flow rates of 2.68, 2.67, and 2.66 mg/s.

radiative heat loss, and the results were indistinguishable near the transport-induced limit, suggesting that system heat loss is not only unnecessary for oscillations in spherical diffusion flames, but it also does not affect the behavior of oscillation. Also shown in the figure is the maximum temperature of a flame at the steady-state turning point ($m = 2.647$ mg/s) as determined in Fig. 1. It appears that once the maximum flame temperature drops below this critical value during the course of oscillation, the flame cannot recover and extinction occurs.

Figure 3 shows an example of a flame at a mass flow rate just beyond the onset of instability ($m = 2.677$ mg/s). The flame oscillates for a relatively long time, over 320 cycles (460s), before eventually extinguishing. The large amplitude of temperature oscillations (almost 50 K before extinction), along with the lengthy duration, suggests that this instability could very likely be observed under microgravity conditions in experiments of sufficient duration. Again, the oscillation grows in amplitude until the maximum flame temperature falls below that at the steady-state extinction turning point, at which time the flame cannot recover and extinction occurs precipitously.

Figure 4 shows the location of both the maximum temperature and the maximum heat release rate for the oscillatory extinction case of $m = 2.67$ mg/s. Although they both fluctuate, the movement is relatively small until extinction occurs, especially for the location of the maximum heat release rate. This flame

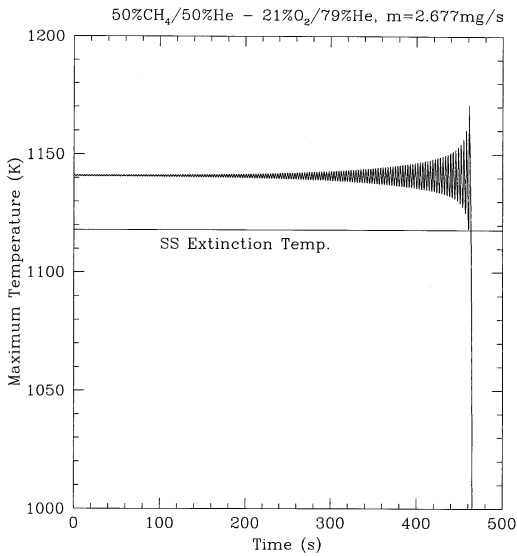


Fig. 3. Maximum temperature as a function of time for a methane diffusion flame with a mass flow rate of 2.677 mg/s.

has a thickness of about 6 mm (based on the width of the heat release rate profile at half its maximum), while the location of the maximum heat release rate moves less than 1 mm during each cycle of oscillation. Therefore, even though the flame experiences unsteady burning, it appears that the location of the flame would exhibit minimal movement visually.

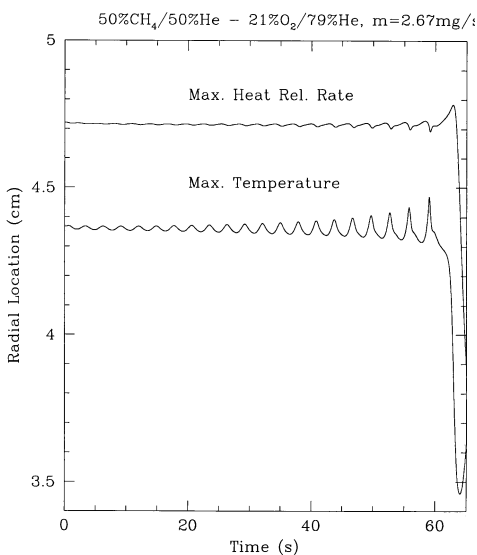


Fig. 4. Location of maximum temperature and maximum heat release rate vs. time for a methane diffusion flame with a mass flow rate of 2.67 mg/s.

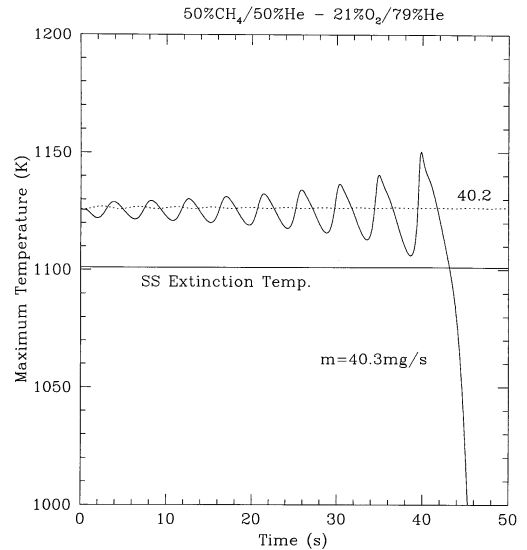


Fig. 5. Maximum temperature as a function of time for methane diffusion flames with mass flow rates of 40.2 and 40.3 mg/s.

This signifies that an experimental identification of an oscillating behavior should rely more on detecting pulsations in the flame temperature or luminosity rather than the flame location itself.

The stability of the methane diffusion flame near the radiation-induced extinction limit was investigated in the same manner. The behavior was similar to the low mass flow rate results; a critical mass flow rate was found which separated stable from unstable flames. Figure 5 shows a flame with a mass flow rate of 40.2 mg/s in which a small perturbation is damped out. However, for $m = 40.3$ mg/s, oscillation develops and grows until flame extinction. Again, as the magnitude of oscillation grows and the maximum temperature drops below the maximum temperature at the steady-state extinction limit (in this case, for $m = 48.7$ mg/s, the radiation-induced turning point), the flame cannot recover and extinction occurs. The frequency of oscillation is lower than that at the smaller mass flow rate for this radiative, lower-characteristic temperature flame (about 0.25 Hz), which is expected as the results of Refs. [11,12] show that the period of oscillation should scale with the characteristic flame time. Note that the oscillation frequencies between the transport-limited and radiation-limited cases are close because the basic flame structures are similar. The relevant parameter here is the canonical Da of Liñán rather than the system Da based on the flame radius. The flame radius only affects total radiative loss and in turn the temperature field, thereby moderately influencing the flame thickness.

Figure 6 shows the location of the maximum

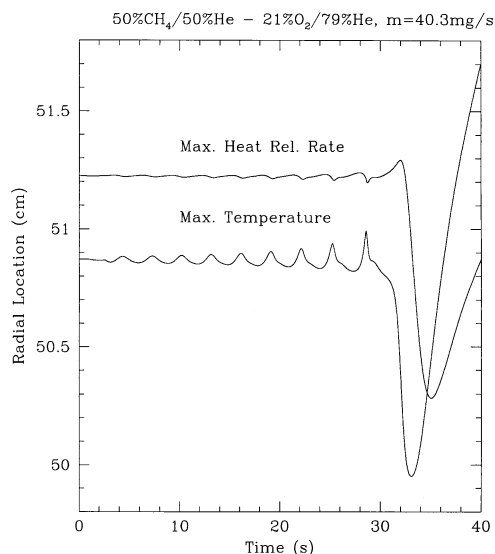


Fig. 6. Location of maximum temperature and maximum heat release rate vs. time for a methane diffusion flame with a mass flow rate of 40.3 mg/s.

temperature and the maximum heat release rate for the oscillatory extinction case of $m = 40.3$ mg/s. Again, both locations fluctuate, but the movement is relatively small, especially for this very large flame. The location of the maximum heat release rate barely moves until the flame extinguishes.

The critical mass flow rate required to trigger the onset of oscillation was investigated further in order to determine if stable limit cycles could exist. However, no limit cycles were observed near the onset of oscillation for either the transport- or radiation-induced limits. If the mass flow rate is in close vicinity of the onset of oscillation, the growth rate of oscillation can be very small, but eventually the oscillation becomes large enough to extinguish the flame. This behavior is different from that observed by Sohn et al. [14], where a very small regime in Da of the limit cycle behavior was found near the radiation-induced limit. This discrepancy could possibly be due to the difference in geometry between these two studies, since the volumetric heat loss is proportional to the cube of a perturbation to the flame size in the spherical flames, while it is only linearly proportion in the planar flames. It is also possible that the limit cycle behavior only exists in an extremely narrow regime, and was missed in our scanning, or that the duration of simulation in Ref. [14] was limited so that extinction was not reached. Figure 3 does demonstrate that it is possible for a flame to oscillate for an extremely long time before extinction occurs.

It is worth noting again the large size of the flame

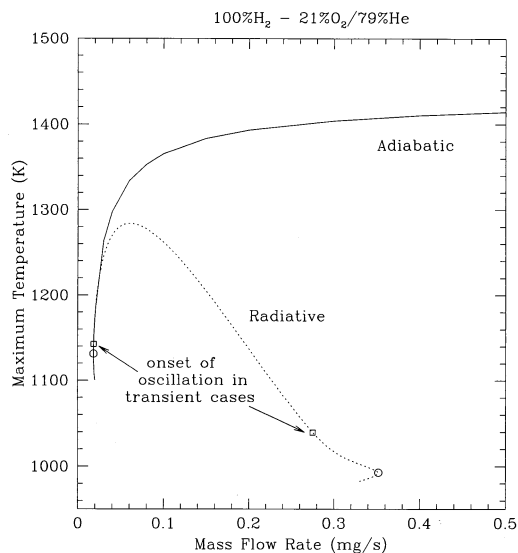


Fig. 7. Maximum temperature as a function of mass flow rate for adiabatic and radiative hydrogen diffusion flames.

near the radiation-induced limit. For simplicity in presenting the role of radiative heat loss on the dynamics of flame instability, the results given are based on optically thin assumptions. At such large flame sizes though, and with the presence of a strong absorber such as CO_2 , gas-phase radiative re-absorption effects should be important. Limited calculations revealed that gas-phase re-absorption does quantitatively modify the transition boundaries (allowing for even larger resultant flames, thereby affecting oscillation frequencies as well), but does not really qualitatively alter the features described. Radiative re-absorption mapping calculations are computationally intensive; their impact on flame stability due to flame structure alterations is the subject of future work.

3.2. Hydrogen diffusion flames

3.2.1. Steady-state response

We will now discuss results for 100% H_2 into 21% O_2 /79%He diffusion flames. Again, the maximum flame temperature curves for both steady-state adiabatic flames and those with radiative heat loss are plotted vs. the mass flow rate in Fig. 7. As in the methane flames, in the absence of heat loss, transport induced extinction occurs as the mass flow rate is reduced, while the maximum temperature monotonically increases as the mass flow rate is increased. The radiative flame response is similar to the methane results, exhibiting radiative extinction at high mass flow rates and transport-induced extinction at

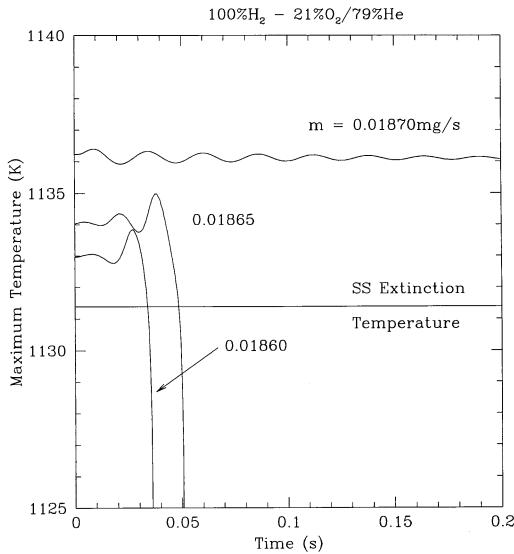


Fig. 8. Maximum temperature as a function of time in hydrogen diffusion flames with mass flow rates of 0.01870, 0.01865, and 0.01860 mg/s.

low mass flow rates, where it is once again indistinguishable from the adiabatic curve.

3.2.2. Transient response

Oscillations were also observed in near-limit hydrogen diffusion flames; however, they appear substantially different from the oscillations of the methane diffusion flames. Figure 8 shows the transient response of the maximum flame temperature in transport-induced limit hydrogen flames with three different mass flow rates: 0.01870, 0.01865, and 0.01860 mg/s. Such a fine resolution in mass flow rate was necessary to observe oscillation in this flame. Once again, a 0.1% perturbation was applied to the temperature profile in order to test the stability of the flames. The two smaller mass flow rates experience oscillation, which quickly leads to extinction. For $m = 0.01870$ mg/s, a small oscillation starts to grow and is then damped out as the flame approaches steady state. The maximum temperature at the steady-state extinction limit ($m = 0.01850$ mg/s) is also plotted in Fig. 8. As in the methane case, the oscillating flame extinguishes after the maximum temperature falls below the maximum temperature at the steady-state extinction turning point.

It is worth noting that the frequency of the oscillations in these mixtures is about 60 Hz, which is much higher than the frequency of oscillation in the methane flames. Compared to the oscillations observed in methane flames, the amplitude of oscilla-

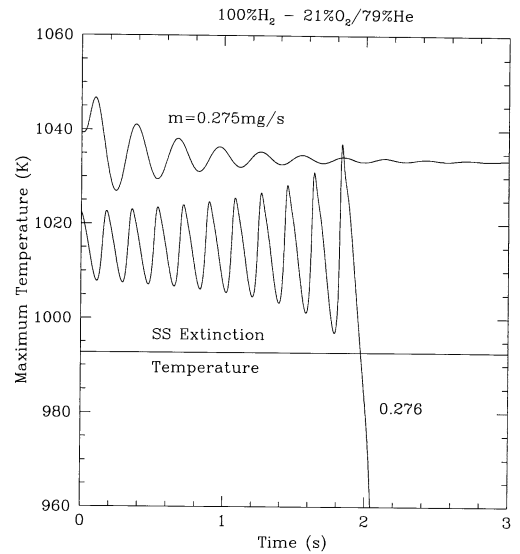


Fig. 9. Maximum temperature as a function of time in hydrogen diffusion flames with mass flow rates of 0.275 and 0.276 mg/s.

tion is much lower and the duration of oscillation is much shorter with an infinitesimal range of oscillatory mass flow rates.

Near the radiation-induced extinction limit a similar oscillation leading to extinction was also observed in hydrogen diffusion flames. Figure 9 shows the maximum temperature as a function of time for $m = 0.275$ and 0.276 mg/s. For a mass flow rate of 0.275 mg/s, the initial perturbation is damped out and the flame approaches the steady-state solution. However, for $m = 0.276$ mg/s, an oscillation develops which results in the extinction of the flame. This oscillation leading to extinction is more similar to the methane oscillations than it is to the oscillations observed near the transport-induced limit in hydrogen flames, having a smaller characteristic frequency and sustaining a larger number of oscillations before extinguishing. Once again, the maximum temperature of the transient flame crosses the maximum temperature of the steady-state extinction turning point as it extinguishes.

3.3. Mechanism for oscillation and extinction

We now discuss the mechanism driving the oscillations in these diffusion flames by closely analyzing the near transport-induced limit case in methane flames ($m = 2.67$ mg/s). Recall from the above results that, although the location of the maximum heat release remains relatively fixed, the magnitude of the heat release rate, however, can vary by a large

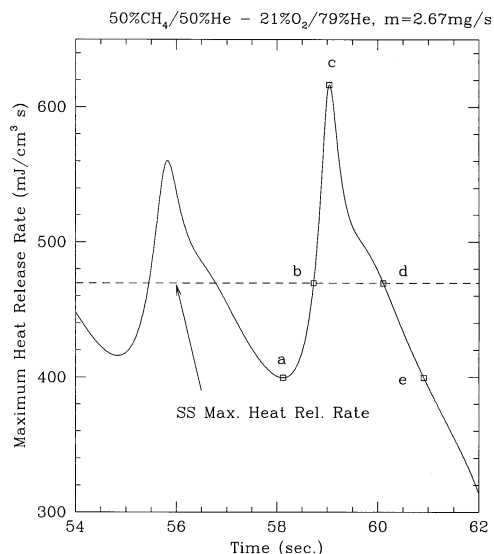


Fig. 10. Maximum heat release rate as a function of time for a methane diffusion flame with a mass flow rate of 2.67 mg/s.

amount during the cycle of oscillation. Figure 10 shows the maximum heat release rate during the last couple of cycles of oscillation before extinction, for $m = 2.67$ mg/s. The amplitude of oscillation during the last cycle is 35% of the steady-state value of the maximum heat release rate.

In order to better understand the nature of the oscillation, as well as the events leading to extinction, five points along a cycle of oscillation are marked in Fig. 10 as “a,” “b,” “c,” “d,” and “e.” Point a corresponds to the smallest maximum heat release rate before the last oscillation, and point e is at the same value, but after the last cycle. Points b and d are at the same value of maximum heat release rate as the steady-state flame, and point c is at the top of the last oscillation. These five points during the last cycle will also be referenced in the next three figures.

The maximum heat release rate is plotted again in Fig. 11, but rather as a function of the mass flow rate at the point of maximum heat release rate normalized by the mass flow rate from the burner ($m = 2.67$ mg/s). It is seen that the flame response spirals outwards from the initial conditions in a counter-clockwise direction until the flame extinguishes and the heat release falls off. Furthermore, as the heat release increases (a to c), the mass flow rate through the flame increases, and correspondingly as the heat release decreases (c to e), the mass flow rate also decreases. This behavior is due to thermal expansion in the flame; as the heat release (and hence temperature) increases, the local density decreases and the

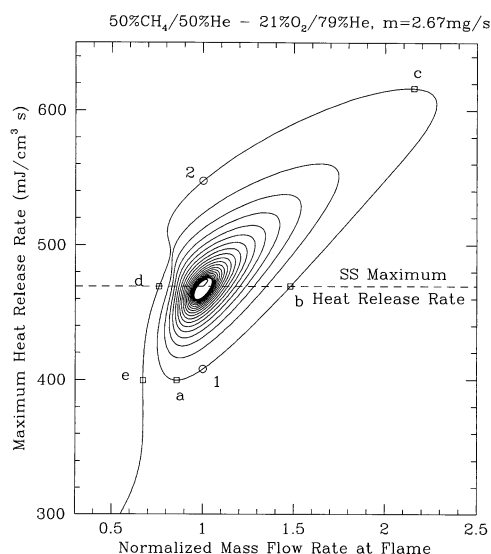


Fig. 11. Maximum heat release rate vs. normalized mass flow rate at the point of maximum heat release rate for an oscillating methane diffusion flame with a mass flow rate of 2.67 mg/s.

mass flux through the flame must increase in order to conserve mass. It is interesting to note that this is the opposite of what one would expect if the flame behaved in a quasi-steady manner (where the heat release would decrease with increasing mass flow rate). This behavior illustrates the purely unsteady nature of this instability. Figures 12 and 13 show the velocity and temperature profiles respectively at the instants a through e. It can be seen that a small change in the maximum temperature ($\sim 4\%$) can lead to a large change in the velocity through the flame ($\sim 200\%$).

When the flame reaches point c, the increased burning rate cannot be sustained for two reasons: the flame is consuming the fuel at a greater rate than it is introduced to the system, and the greater velocity through the reaction zone reduces the residence time (and hence Da), resulting in a decreasing burning rate. As the flame goes through the downward part of the cycle (c to e), the reverse occurs: the heat release decreases, the temperature decreases, the density increases and the velocity through the flame decreases. As the consumption rate of the reactants falls below the steady-state rate, excess reactants build up in the system. Eventually, a point is reached where the excess reactants and the longer residence time (due to the decrease in velocity) cause the burning rate to increase once again despite the low temperature and the cycle repeats itself. However, as the oscillations grow in amplitude with each cycle, the maximum temperature (which is an intrinsic indicator of the

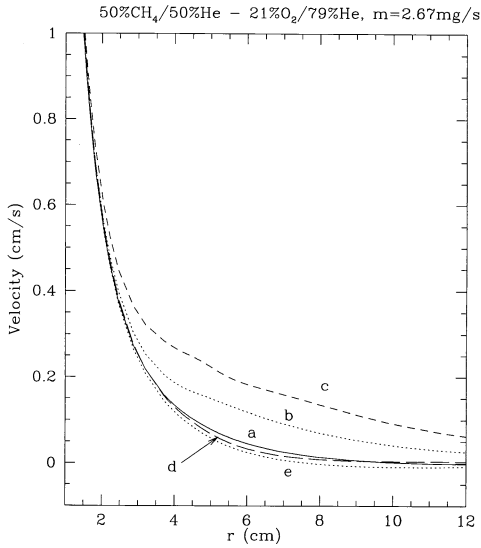


Fig. 12. Velocity profiles for an oscillating methane diffusion flame with a mass flow rate of 2.67 mg/s at (a) $t = 58.12$, (b) 58.73, (c) 59.04, (d) 60.11 and (e) 60.91 s.

enthalpy structure) eventually drops below the steady-state extinction temperature (as shown in Figs. 2 and 3), and the flame is unable to recover and extinction occurs.

The additional points “1” and “2” in Fig. 11 mark instances along the cycle of oscillation where the mass flow rate through the flame is equal to the mass

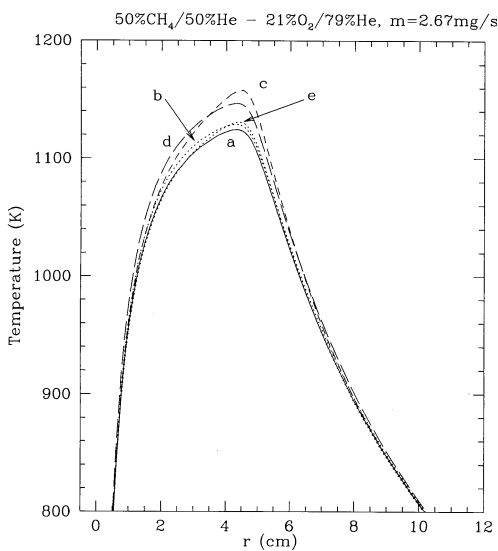


Fig. 13. Temperature profiles for an oscillating methane diffusion flame with a mass flow rate of 2.67 mg/s at $t =$ (a) 58.12, (b) 58.73, (c) 59.04, (d) 60.11, and (e) 60.91 s.

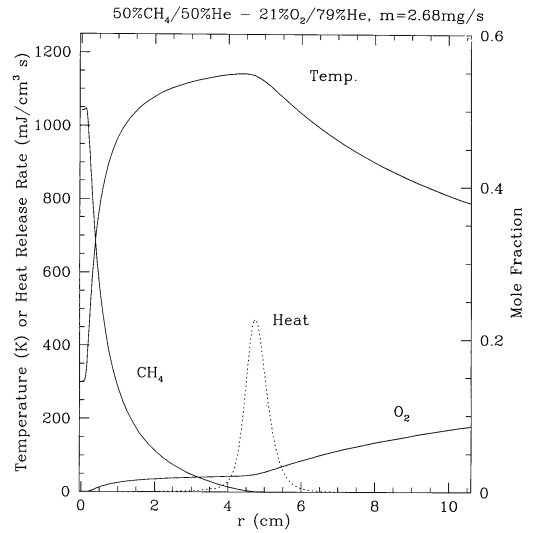


Fig. 14. Structure of a methane diffusion flame with a mass flow rate of 2.68 mg/s.

flow rate from the point source, yet they correspond to very different values of the maximum heat release rate. The difference here is due to fuel accumulation and depletion in the reaction zone during the lower and upper portions of the cycle respectively, and is responsible for the hysteresis in the curves of Fig. 11.

3.4. Comparison of flame structure

In order to obtain a better understanding of the differences between the oscillations in the two fuels, we have plotted the temperature, heat release rate, and fuel and oxidizer mole fraction profiles for the methane and hydrogen flames in Figs. 14 and 15, respectively. Both figures show the flame structure of the steady-state solution just before the onset of oscillation ($m = 2.68$ mg/s for methane and $m = 0.01870$ mg/s for hydrogen) near the transport-induced extinction limit. It is seen that the methane flame exhibits a typical flame structure characteristic of a diffusion flame with high activation energy. The narrow heat release zone is confined to a region of high temperature where the fuel is rapidly consumed. The temperature profile is very broad compared to the species profiles, which is indicative of a $Le > 1$ behavior. There is substantial reactant leakage through the flame, which is expected because of the close proximity to the extinction limit.

The hydrogen flame structure, however, is distinctly different from the methane flame. The heat release zone is very broad, and the temperature profile does not contain the well-defined peak as in the methane flame. There is significant overlap of hydro-

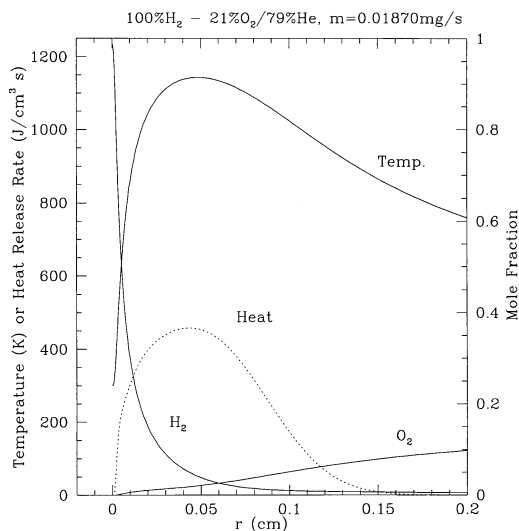


Fig. 15. Structure of a hydrogen diffusion flame with a mass flow rate of 0.018105 mg/s.

gen and oxygen within the flame. This structure is due to the large mass diffusivity of hydrogen. In fact, the reaction zone resembles that of a premixed flame instead of a diffusion flame, especially considering that the flammability limits of premixed hydrogen flames can be extremely broad. In fact, the frequency of oscillation of 60 Hz is comparable to the pulsating instability observed in rich premixed hydrogen/air flames [15,16].

The flame structure at the onset of oscillation near the radiation-induced extinction limit is shown for both the methane ($m = 40.3$ mg/s) and hydrogen ($m = 0.275$ mg/s) flames in Figs. 16 and 17, respectively. It is seen that the methane flame is extremely large (maximum heat release occurs at a radius of 58 cm), with the heat release region confined to a very narrow reaction zone within the flame structure. Such a large flame would be difficult to observe experimentally without any interactions with the surroundings.

The hydrogen flame structure is similar to that at the low mass flow rate, transport-induced extinction limit, despite its larger size. The heat release zone is still broader than that of the methane flame, although not as dramatically as in the low mass flow rate flame.

4. Concluding remarks

The steady-state and transient responses of spherically symmetric helium-diluted methane and hydrogen diffusion flames were numerically simulated us-

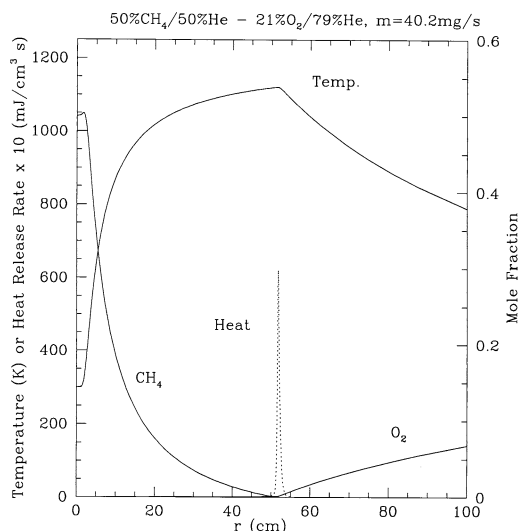


Fig. 16. Structure of a methane diffusion flame with a mass flow rate of 40.2 mg/s.

ing detailed chemistry and transport, with and without radiative heat loss. Both the radiative and non-radiative steady-state results exhibited extinction limits at small mass flow rates corresponding to sufficiently short residence times through the small flames. At large mass flow rates, radiation-induced extinction limits were observed that are not present in the non-radiative flames.

The methane and hydrogen flames exhibited oscillatory behavior near both extinction limits. How-

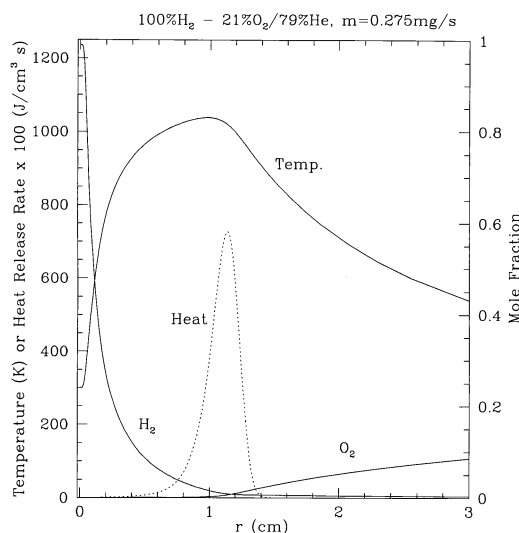


Fig. 17. Structure of a hydrogen diffusion flame with a mass flow rate of 0.285 mg/s.

ever, the oscillations are qualitatively different between the two fuel mixtures; the methane flame exhibits large amplitude temperature fluctuations at a frequency of about 0.35 Hz, while the hydrogen flames experienced relatively small amplitude oscillations with a frequency of about 60 Hz, resulting from their distinctively different flame structures. The oscillations in the methane flame appear to be similar and compare qualitatively well to those predicted analytically by Cheatham and Matalon [12], while the oscillations in the hydrogen flame are similar to those observed in rich premixed hydrogen/air flames [15,16].

Neither mixture exhibits oscillation that developed into a stable limit cycle; either the oscillation grows until it becomes large enough to extinguish the flame, or the oscillation diminishes as the flame returns to the steady-state solution. However, the oscillations in methane flames last longer than 320 cycles at some mass flow rates, suggesting this behavior could possibly be observed experimentally.

Acknowledgments

This work was supported by the AFOSR and National Aeronautics and Space Administration (NASA). The authors would like to acknowledge helpful discussions with Professor Yiguang Ju of Princeton University.

References

- [1] B.H. Chao, C.K. Law, J.S. Tien, Twenty-Third Symposium (International) on Combustion (1993) pp. 523–531, The Combustion Institute, Pittsburgh.
- [2] K. Mills, M. Matalon, Twenty-Seventh Symposium (International) on Combustion, The Combustion Institute, Pittsburgh, 1998, pp. 2535–2541.
- [3] B.H. Chao, C.K. Law, *Combust. Flame* 92 (1993) 1–24.
- [4] Dietrich, D.L., Ross, H.D., Frante, D.T., Tien, J.S. Shu, Y., 4th Int. Microgravity Combustion Workshop, Cleveland, OH, NASA Conference Publication No. 10194, 1997.
- [5] V. Nayagam, F.A. Williams, Seventh International Conference on Numerical Combustion, York, England, 1998.
- [6] M. Fűri, P. Papas, P.A. Monkewitz, *Proc. Combust. Inst.* 28 (2000) 831–838.
- [7] L.L. Kirkby, R.A. Schmitz, *Combust. Flame* 10 (1966) 205–220.
- [8] J.S. Kim, *Combust. Theory Modelling* 1 (1997) 13–40.
- [9] A. Liñán, *Acta Astronautica* 1 (1974) 1007–1039.
- [10] G.I. Sivashinsky, *Int. Heat Mass Transfer* 17 (1974) 1499–1506.
- [11] S. Cheatham, M. Matalon, Twenty-Sixth Symposium (International) on Combustion, The Combustion Institute, Pittsburgh, 1996, pp. 1063–1070.
- [12] S. Kukuck, M. Matalon, *Combust. Theory Modelling* 5 (2001) 217–240.
- [13] C.H. Sohn, S.H. Chung, J.S. Kim, *Combust. Flame* 117 (1999) 404–412.
- [14] C.H. Sohn, J.S. Kim, S.H. Chung, K. Maruta, *Combust. Flame* 123 (2000) 95–106.
- [15] E.W. Christiansen, C.J. Sung, C.K. Law, *Combust. Flame* 124 (2001) 35–49.
- [16] E.W. Christiansen, C.J. Sung, C.K. Law, Twenty-Seventh Symposium (International) on Combustion, The Combustion Institute, Pittsburgh, 1999, pp. 555–562.
- [17] E.W. Christiansen, C.K. Law, C.J. Sung, *Proc. Combust. Inst.* 28 (2000) 807–814.
- [18] R.J. Kee, J.F. Grcar, M.D. Smooke, J.A. Miller, A Fortran program for modeling steady laminar one-dimensional premixed flames, Report No. SAND85-8240, Sandia National Laboratories, 1985.
- [19] C.L. Tien, *Adv. Heat Transfer* 5 (1967) 253.
- [20] R.K. Hanson, D.F. Davidson, E.J. Chang, G.P. Smith, D.M. Golden, W.C. Gardiner, V. Lissianski, <http://www.me.berkeley.edu/gri-mech/>, 1995.
- [21] M.A. Mueller, T.J. Kim, R.A. Yetter, F.L. Dryer, *Int. J. Chem. Kinet.* 31 (1999) 113–125.